

Anomalous avoided level crossings in a Cooper-pair box spectrum

Z. Kim,^{1,2} V. Zaretsky,^{1,2} Y. Yoon,² J. F. Schneiderman,³ M. D. Shaw,³ P. M. Echternach,⁴ F. C. Wellstood,^{2,5} and B. S. Palmer^{1,*}

¹*Laboratory for Physical Sciences, College Park, Maryland, 20740*

²*Department of Physics, University of Maryland, College Park, Maryland, 20742*

³*Department of Physics, University of Southern California,
Los Angeles, California 90089-0484*

⁴*Jet Propulsion Laboratory, California Institute of Technology, Pasadena, California, 91109*

⁵*Joint Quantum Institute and Center for Nanophysics and Advanced Materials*

(Dated: October 30, 2018)

Abstract

We have observed a few distinct anomalous avoided level crossings and voltage dependent transitions in the excited state spectrum of an Al/AlO_x/Al Cooper-pair box (CPB). The device was measured at 40 mK in the 15 - 50 GHz frequency range. We find that a given level crosses the CPB spectrum at two different gate voltages; the frequency and splitting size of the two crossings differ and the splitting size depends on the Josephson energy of the CPB. We show that this behavior is not only consistent with the CPB being coupled to discrete charged “two-level” quantum systems which move atomic distances in the CPB junctions but that the spectra provide new information about the fluctuators, which is not available from phase qubit spectra of anomalous avoided levels. In particular by fitting a model Hamiltonian to our data, we extract microscopic parameters for each fluctuator, including well asymmetry, tunneling amplitude, and the minimum hopping distance for each fluctuator. The tunneling rates range from less than 3.5 to 13 GHz, which represent values between 5% and 150% of the well asymmetry, and the dipole moments give a minimum hopping distance of 0.3 to 0.8 Å. We have also found that these discrete two-level systems have a pronounced effect on the relaxation time (T_1) of the quantum states of the CPB and hence can be a source of dissipation for superconducting quantum bits.

PACS numbers: 85.25.Cp and 85.35.Gv

Two-level fluctuators (TLF) of one kind or another have long been recognized as an underlying cause of resistance fluctuations in metals,^{1,2} critical current fluctuations in Josephson junctions,^{3,4,5,6,7} excess flux noise in SQUIDs,^{7,8,9} and telegraph noise and excess charge noise in Coulomb blockade devices.^{10,11,12,13} For charge and critical current fluctuations - the fluctuators appear to be moving charges or rotating electric dipoles in the insulating junction barrier or nearby dielectric layers³ - but the precise microscopic identification of the fluctuators is not settled.

There are several reasons why it has been difficult to be certain of the precise microscopic agents causing charge or critical current fluctuations. First, the effects from individual fluctuators are typically very small, especially for the cryogenic or milli-Kelvin temperatures of interest here, and this typically makes the resulting experiments quite challenging. Second, a variety of materials and processes have been used to build devices, and the presence of a fluctuator may well depend on both the materials and the fabrication technique. Third, while measurements of telegraph noise can reveal microscopic information about individual fluctuators, in many cases it is possible only to distinguish the largest one or two fluctuators in a background noise of smaller fluctuations. Compared to the number of atoms in even the smallest device, such observable discrete fluctuators are extremely rare and thus may not be representative of a typical atomic scale defect in the device. Finally, much of the experimental data obtained on fluctuators consists of relatively smooth $1/f$ noise power spectra. Such noise spectra arise from a distribution of many fluctuators^{1,14} and it is often not possible to resolve individual fluctuators. From smooth spectra, it is difficult to determine uniquely such basic microscopic parameters as the hopping distance or the absolute number of fluctuators in a given energy range.

Research in quantum computing based on superconducting devices has led to increased interest in understanding two-level fluctuators. In qubit research, fluctuators can be a serious problem because they can lead to decoherence, dissipation, inhomogeneous broadening and a decrease in measurement fidelity.^{15,16,17,18,19,20} With this new interest have also come new approaches to the problem. In particular, microwave spectroscopy of the various superconducting qubits has revealed the presence of small un-intended avoided crossings in the transition spectrum due to coupling between the device and individual two-level fluctuators.^{15,16,18,19,20,21} Avoided level crossings were initially seen in the phase qubit¹⁵ and subsequently in the flux qubit^{18,20}, quantronium¹⁹, and the transmon.²¹ While it was initially

thought that the anomalous avoided level crossings were due to critical current fluctuations,¹⁵ a later comparison of a hopping distance (extracted from an analysis of an ensemble of avoided level crossings) to atomic distances suggested that charge fluctuators were responsible.¹⁶

In this article, we report observations of anomalous avoided level crossings in the transition spectrum of a Cooper-pair box (CPB), a superconducting quantum device that is sensitive to charge. We find that each avoided level crossing is due to a charged two level system in which the charge moves atomic distances in the tunnel barrier of the device's Josephson junction. The spectra contain a striking feature not seen in phase qubits - the two level system's levels are voltage dependent - and by modeling the full spectrum, we can resolve some of the key microscopic parameters of each fluctuator. We also find a strong correlation between the locations of the avoided level crossings and decreases in the lifetime (T_1) of the excited state of the qubit.

For our measurement, we use a CPB consisting of a small superconducting island connected to superconducting leads by two ultra-small (nominal area 120 nm by 120 nm) Josephson junctions (see Fig. 1). By applying voltage V_g to a gate electrode, which is capacitively coupled to the CPB island with capacitance C_g , we can control the number n of excess Cooper pairs on the island. Neglecting the quasiparticle states,^{22,23} the Hamiltonian describing the CPB is given by^{24,25}

$$\hat{H}_{CPB} = E_c \sum_n (2n - n_g)^2 |n\rangle \langle n| - \frac{E_J}{2} \sum_n (|n+1\rangle \langle n| + |n\rangle \langle n+1|) \quad (1)$$

where $n_g = -C_g V_g / e$ is the reduced gate voltage, $e = -1.609 \times 10^{-19}$ C is negative, $E_c = e^2 / 2C_\Sigma$ is the charging energy, C_Σ is the total capacitance of the island, and E_J is the Josephson energy. At the CPB charge degeneracy point, which occurs when n_g is an odd integer, the energy difference between the first excited state and ground state is a minimum and approximately E_J . By applying a magnetic flux (ϕ) through the superconducting loop, E_J can be effectively changed by the quantity $E_J = E_J^{Max} \cos(\pi\phi/\phi_o)$ where $E_J^{Max} = \hbar I_c / 2e$, I_c is the critical current of the two junctions, and $\phi_o = hc / 2e$ is the magnetic flux quantum. Similarly, the first and second excited state have a minimum splitting of approximately $E_J^2 / 16E_c$ and this minimum occurs at even values of n_g .

To measure the excess charge on the CPB, we used a superconducting Coulomb-blockade electrometer that is capacitively coupled to the CPB [see Fig. 1(a)].²⁶ The electrometer

and the CPB were formed together on a quartz substrate in the same process; we used electron beam lithography and standard double-angle evaporation of Al with an oxidation step to form an AlO_x tunnel barrier between the two Al layers.²⁷ To improve the bandwidth of the measurement, the electrometer was connected to an on-chip LC tank circuit and operated in an rf-SET mode;²⁸ the reflectance was measured at the resonance frequency of the tank circuit (640 MHz) while the electrometer was dc biased at the Josephson quasiparticle resonance and with the gate of the electrometer tuned to maximize the sensitivity to charge changes.²⁹

The sample was mounted in a Cu box that was bolted to the mixing chamber of an Oxford Instruments model 100 dilution refrigerator with a base temperature of 40 mK. Figure 2 shows a plot of the measured change in the rf reflectance of the rf-SET as a function of n_g and frequency of a microwave perturbation applied to the gate of the CPB. For this plot, the microwave frequency was adjusted between 24 and 50 GHz in steps of 30 MHz. When the applied frequency is resonant with a level splitting of the CPB, the CPB state changes, causing a change in the charge on the island, which causes a change in the reflectance of the rf-SET. The white parabolic like band between $0 < n_g < 1$ in Fig. 2 corresponds to a measured change of $\approx 1e$ on the island of the CPB while the black parabola between $1 < n_g < 2$ corresponds to a measured change of $\approx -1e$ on the island of the CPB.

Close examination of the spectrum reveals a few small avoided crossings which are not predicted by Eq. 1; anomalous avoided crossings imply that additional degrees of freedom are coupled to the CPB. Figure 3 shows a detailed view of the spectrum near two prominent avoided crossings due to a single fluctuator for four different values of E_J . In Fig. 3(a), one crossing occurs at $f = 34.3$ GHz and $n_g = -0.43$. A second crossing occurs at $f = 33.5$ GHz and $n_g = 0.48$. We note in particular the presence near each crossing of short features in the spectrum that appear to point toward the other crossing (see arrows in Fig. 3a which indicate small projections in the spectrum), suggesting the two crossings are related. When n_g was swept over multiple periods, we found that this spectrum was periodic with period 2. Figures 3(a) through 3(d) show that the spectrum changes as E_J/k_B is decreased from 1.0 K to 0.1 K. In particular as E_J is reduced, the avoided crossing splitting decreases from a size of 150 MHz to a size that is too small for us to determine. The other anomalous avoided crossings we observed showed similar behavior.

The dependence of the crossings on gate voltage and Josephson energy are consistent with

the CPB being coupled to a charged fluctuator that is moving in one of the Al/AlO_x/Al ultra-small junction barriers. In particular, because the avoided level crossings have a periodicity of 2 in reduced gate voltage, this suggests that the charge fluctuator resides in one of the two tunnel junctions that form the CPB; the electrostatic potential of the CPB island is given by $V_i = e/C_\Sigma(2n - n_g)$ which has a periodicity of 2 in n_g for the different states of the CPB.

In general, the Hamiltonian for a charged fluctuator would depend on the local environment including other charged defects in the system. To simplify the problem, we assume that the fluctuator takes the form of a point charge moving between two potential wells. In this approximation the Hamiltonian for the TLF is

$$\hat{H}_{TLF} = \varepsilon_a |x_a\rangle \langle x_a| + \varepsilon_b |x_b\rangle \langle x_b| + T_{ab}(|x_a\rangle \langle x_b| + |x_b\rangle \langle x_a|) \quad (2)$$

where ε_a is the energy of the fluctuator at position x_a , ε_b is the energy of the fluctuator at position x_b , and T_{ab} is the tunneling matrix element between the two sites. For an isolated fluctuator, the difference in energy between the two states of the TLF is given by $\sqrt{(\varepsilon_b - \varepsilon_a)^2 + 4T_{ab}^2}$.

Assuming the fluctuator is a point charge that resides in the tunnel junction, with charge Q_{TLF} , the change in the induced polarization charge on the island of the CPB when the fluctuator tunnels from position x_a to x_b is given by $\Delta Q_{pi} = Q_{TLF}(x_b - x_a) \cos(\eta)/d$ where η is the angle of displacement relative to the electric field in the junction and d is the thickness of the tunnel junction.³⁰ Since the charge on the island is constant when n is constant, a corresponding change in the polarization charge ($-\Delta Q_{pi}$) must exist over the rest of the island. This in turn induces a change in the induced surface charge on the gate electrode given by $\Delta Q_g = \Delta Q_{pi} C_g / C_\Sigma$. Finally, we find that the change in the electrostatic potential of the island due to motion of the point charge is given by³¹

$$\Delta V_i = \frac{Q_{TLF}}{C_\Sigma} \frac{(x_b - x_a) \cos(\eta)}{d}. \quad (3)$$

Note that the total electrostatic potential of the island depends on the number of excess Cooper-pairs on the island, the displacement of the point charge and the reduced gate voltage. Accounting for the electrostatic charging energy and the work done by gate voltage source when the point charge moves, the following coupling Hamiltonian is found³¹

$$\hat{H}_{CPB-TLF} = 2E_c \sum_{x=x_a, x_b} \sum_n (2n - n_g) \frac{Q_{TLF}}{e} \frac{x \cos(\eta)}{d} |n\rangle |x\rangle \langle x| \langle n|. \quad (4)$$

Combining Eqs. 1, 2, and 4 we find the total Hamiltonian for a CPB coupled to a single fluctuator. From this, we can find the energy levels and the transition frequencies from the ground state to the excited states of the system and fit the measured spectrum. We note that in this model, an avoided crossing occurs when the first excited state of the TLF is resonant with the first excited state of the CPB. The change in the induced polarization charge on the CPB island due to the fluctuator being excited ultimately gives rise to the avoided level crossings at two different frequencies and two different reduced gate voltages (i.e. it breaks the symmetry of the CPB). The splitting size in our model depends on E_J ; coupling the two excited states together is a second order process that involves both the tunneling of a Cooper pair and the tunneling of the TLF. The dashed red curve in Fig. 3 shows the predicted spectrum for the splitting we found near 34 GHz. Here we used fit parameters $(\varepsilon_b - \varepsilon_a)/k_B = 1.427$ K, $T_{ab}/k_B = 0.39$ K, and $Q_{TLF}\delta x \cos(\eta)/ed = -0.074$ where $\delta x = (x_b - x_a)$ is the maximum displacement of the fluctuator. We note that extracting these three parameters requires us to measure the splitting size and frequency of the avoided crossings at two different gate voltages and that these fit parameters can be varied by approximately 10% to maintain a good fit.

We found another prominent avoided crossing near 43 GHz and smaller avoided crossings near 20 and 39 GHz. Table I summarizes the best fit results for all of the observed avoided crossings. The avoided crossing near 39 GHz had a splitting size too small to resolve, which places an upper bound on T_{ab} of the TLF. Assuming a TLF charge of $Q_{TLF} = e$ and a tunnel barrier thickness of $d = 1$ nm, we extract minimum hopping distances for the fluctuators that range from 0.32 Å to 0.83 Å.

The model also predicts state transitions of the TLF at gate voltages away from the observed avoided crossings. Although these were not visible in Fig. 3, we found that weak transitions could be observed far from the avoided crossing when the microwave excitation power was increased by approximately a factor of ten. Figure 4(a) shows the measured excess charge spectrum between an applied frequency of 33 and 34.6 GHz; note the very faint transition due to the TLF between $n_g = -1.25$ and $n_g = -0.75$. In this region the measured excess charge on the CPB is approximately $-0.03 e$, about an order of magnitude smaller than predicted from our simple theory. Figure 4(b) overlays the predicted spectrum using the parameters found in Fig. 3.

Similarly, Fig. 4(c) shows the measured excess charge spectrum between 41.5 to 44.5 GHz;

a frequency range where another prominent avoided crossing was observed. Note that in Fig. 4(c) we observe weak voltage dependent transitions, due to the TLF, near $n_g = 0.8$ and $f = 44.25$ GHz; as well as between $n_g = -0.8$ and -0.4 . Again the predicted spectrum in Fig. 4(d) follows the measured spectrum accurately. In this spectrum, we observe additional features like non-equilibrium quasiparticles which creates the apparent periodicity in n_g of 1,^{22,23} multiple CPB spectra (i.e. spectra parallel to the CPB spectrum) which is interpreted to be due to low frequency charge fluctuators, and horizontal bands which are due to a change in the gain of the Coulomb-blockade electrometer.

We have also measured the lifetime (T_1) of the excited state of the CPB as a function of the transition frequency. For these measurements, the CPB was excited at its zero to one transition frequency, and the charge on the island was continuously monitored as a function of time using the rf-SET after the excitation source was turned off. The measurements were done at a small Josephson energy to decouple the CPB from charge perturbations in the system and hence increase the lifetime of the qubit to a maximum value.^{32,33} Figure 5 shows the measured decay rate (Γ_1) from 15 GHz to 45 GHz at $E_J/k_B = 0.1$ K. Several peaks in the decay rate are evident; we find that when the CPB is in resonance with the TLF, the measured lifetime decreases from a few microseconds to 1 μ s or less. This decrease in T_1 near a resonance was a useful tool for finding some of the avoided crossings. This behavior suggests that the lifetime of these TLFs is smaller than a few microseconds and that the interaction of the CPB with a charged TLF is a source of dissipation for the CPB.³⁴

Finally, to investigate the stability of the TLFs, the device was warmed up to room temperature. After “annealing” at room temperature for 14 days, the device was cooled again to 40 mK. We found an avoided crossing associated with one level in the 20 - 50 GHz range and one peak in the decay rate at the same frequency. The new crossings occurred around $f = 23$ GHz and fitting to the charge model gave: $(\varepsilon_b - \varepsilon_a)/k_B = 0.34$ K, $T_{ab}/k_B = 0.52$ K, and $Q_{TLF}\delta x \cos(\eta)/ed = 0.078$. We also note that the fluctuators observed here were stable after annealing at 4 K for two days or after placing the device in the normal state by applying a 1 T magnetic field for one hour.

In conclusion, we have observed unintended voltage-dependent transitions and avoided level crossings in the excited state spectrum of a CPB, consistent with a charge fluctuator that can tunnel between two locations separated by atomic scale distances in the tunnel junction. Finally, we note that the spectra allow us to extract key microscopic parameters

of the TLF, such as the tunneling matrix element, and test some theories of fluctuators in these devices.^{3,35,36}

Acknowledgments

This research was supported by the National Security Agency. The authors would like to thank E. Tiesinga, R. Simmonds and K. Osborn for many useful discussions of microstates. FCW would like to acknowledge support from the Joint Quantum Institute and the State of Maryland through the Center for Nanophysics and Advanced Materials.

* Electronic address: bpalmer@lps.umd.edu

- ¹ P. Dutta, P. Dimon, and P. M. Horn, *Phys. Rev. Lett.* **43**, 646 (1979).
- ² C. T. Rogers and R. A. Buhrman, *Phys. Rev. Lett.* **55**, 859 (1985).
- ³ M. Constantin and C. C. Yu, *Phys. Rev. Lett.* **99**, 207001 (2007).
- ⁴ Michael Mück, Matthias Korn, C. G. A. Mugford, J. B. Kycia and John Clarke, *Appl. Phys. Lett.* **86**, 012510 (2005).
- ⁵ F. C. Wellstood, C. Urbina, and John Clarke, *Appl. Phys. Lett.* **85**, 5296 (2004).
- ⁶ D. J. Van Harlingen, T. L. Robertson, B. L. T. Plourde, P. A. Reichardt, T. A. Crane, and J. Clarke, *Phys. Rev. B* **70** 064517 (2004).
- ⁷ R. H. Koch, J. Clarke, W. M. Goubau, J. M. Martinis, C. M. Pegrum and D. J. Harlingen, *J. Low Temp. Phys.* **51**, 207 (1983).
- ⁸ I. Chiorescu, Y. Nakamura, C. J. P. M. Harmans, and J. E. Mooij, *Science* **299**, 1869 (2003).
- ⁹ Y. A. Pashkin, T. Yamamoto, O. Astafiev, Y. Nakamura, D. V. Averin, and J. S. Tsai, *Nature* **421**, 823 (2003).
- ¹⁰ L. J. Geerligs, V. F. Anderegg, J. E. Mooij, *Physica B* **165**, 973 (1990).
- ¹¹ G. Zimmerli, T. M. Eiles, R. L. Kautz, and J. Martinis, *Phys. Lett.* **61**, 237 (1992).
- ¹² L. Ji, P. D. Dresselhaus, S. Han. K. Lin, W. Zheng and J. E. Lukens, *J. Vac. Sci. Technol. B.* **12**, 3619 (1994).
- ¹³ M. Kenyon, C. J. Lobb, and F. C. Wellstood, *J. Appl. Phys.* **88**, 6536 (2000).
- ¹⁴ S. Machlup, *J. Appl. Phys.* **25**, 341 (1954).

- ¹⁵ R. W. Simmonds, K. M. Lang, D. A. Hite, S. Nam, D. P. Pappas, and J. M. Martinis, Phys. Rev. Lett. **93**, 077003 (2004).
- ¹⁶ J. M. Martinis, K. B. Cooper, R. McDermott, M. Steffen, M. Ansmann, K. D. Osborn, K. Cicak, S. Oh, D. P. Pappas, R. W. Simmonds, and C. C. Yu, Phys. Rev. Lett. **95**, 210503 (2005).
- ¹⁷ L. Tian and R. W. Simmonds, Phys. Rev. Lett. **99**, 137002 (2007).
- ¹⁸ B. L. T. Plourde, T. L. Robertson, P. A. Reichardt, T. Hime, S. Linzen, C.-E. Wu, and John Clarke, Phys. Rev. B **72**, 060506(R) (2005).
- ¹⁹ G. Ithier, E. Collin, P. Joyez, P. J. Meeson, D. Vion, D. Esteve, F. Chiarello, A. Shnirman, Y. Makhlin, J. Schrieffer, and G. Schön, Phys. Rev. B **72**, 134519 (2005).
- ²⁰ F. Deppe, M. Mariani, E. P. Menzel, S. Saito, K. Kakuyanagi, H. Tanaka, T. Meno, K. Semba, H. Takayanagi, and R. Gross, Phys. Rev. B **76**, 214503 (2007).
- ²¹ J. A. Schreier, A. A. Houck, Jens Koch, D. I. Schuster, B. R. Johnson, J. M. Chow, J. M. Gambetta, J. Majer, L. Frunzio, M. H. Devoret, S. M. Girvin, and R. J. Schoelkopf, Phys. Rev. B **77**, 180502(R) (2008).
- ²² B. S. Palmer, C. A. Sanchez, A. Naik, M. A. Manheimer, J. F. Schneiderman, P. M. Echternach, and F. C. Wellstood, Phys. Rev. B **76**, 054501 (2007).
- ²³ J. Aumentado, M. Keller, J. Martinis, and M. Devoret, Phys. Rev. Lett. **92**, 066802 (2004).
- ²⁴ M. Büttiker, Phys. Rev. B **36**, 3548 (1987).
- ²⁵ V. Bouchiat, D. Vion, P. Joyez, D. Esteve, and M. H. Devoret, Phys. Script. **T76**, 165 (1998).
- ²⁶ K. Bladh, T. Duty, D. Gunnarsson, and P. Delsing, New Journal of Physics **7**, 180 (2005).
- ²⁷ T. A. Fulton and G. J. Dolan, Phys. Rev. Lett. **59**, 109 (1987).
- ²⁸ R. J. Schoelkopf, P. Wahlgren, A. A. Kozhevnikov, P. Delsing, and D. E. Prober, Science **280**, 1238 (1998).
- ²⁹ T. A. Fulton, P. L. Gammel, D. J. Bishop, L. N. Dunkleberger, and G. J. Dolan, Phys. Rev. Lett. **63**, 1307 (1989).
- ³⁰ J. D. Jackson, *Classical Electrodynamics*, 2nd ed. (John Wiley & Sons, New York, 1975), p. 51.
- ³¹ F. C. Wellstood, Z. Kim, and B. S. Palmer, arXiv:0805.4429 (2008).
- ³² O. Astafiev, Yu. A. Pashkin, Y. Nakamura, T. Yamamoto, and J. S. Tsai, Phys. Rev. Lett. **93**, 267007 (2004).
- ³³ R. J. Schoelkopf, A. A. Clerk, S. M. Girvin, K.M. Lehnert, and M. H. Devoret, in Quantum Noise in Mesoscopic Physics, edited by Y. V. Nazarov (Kluwer Academic Publishers, Netherlands,

2003) pp. 175-203; R. J. Schoelkopf, A. A. Clerk, S. M. Girvin, K.M. Lehnert, and M. H. Devoret, arXiv:cond-mat/0210247v1 (2002).

³⁴ K. B. Cooper, Matthias Steffen, R. McDermott, R. W. Simmonds, Seongshik Oh, D. A. Hite, D. P. Pappas, and John M. Martinis, Phys. Rev. Lett. **93**, 180401 (2004).

³⁵ Lara Faoro, Joakim Bergli, Boris L. Altshuler, and Y. M. Galperin, Phys. Rev. Lett. **95**, 046805 (2005).

³⁶ A. M. Zagoskin, S. Ashhab, J. R. Johansson, and Franco Nori, Phys. Rev. Lett. **97**, 077001 (2006).

FIG. 1: (a) Schematic of experimental setup. A rf Coulomb-blockade electrometer measures the charge state and energy spectrum of the Cooper-pair box (CPB). The CPB and electrometer had a charging energy of $E_c/k_B=0.575$ K and $E_{c,E}/k_B=1.1$ K, respectively. (b) Scanning electron micrograph of the device.

FIG. 2: Measured spectrum of CPB when the applied microwave frequency f is adjusted from 24 GHz to 50 GHz with $E_J/k_B= 1.12$ K. The white parabolic like band between $0 < n_g < 1$ corresponds to a measured change of $\approx 1e$ on the island of the CPB while the black parabola between $1 < n_g < 2$ corresponds to a measured change of $\approx -1e$ on the island of the CPB.

FIG. 3: Measured spectrum of CPB around 34 GHz at different Josephson energies as specified in the graphs. The red and blue colors represent the charge on the island corresponding to the excited and ground state of the system, respectively. The arrows in (a) indicate a small projection of the avoided level that appear to point toward one another. The red dashed line is the predicted spectrum using a Hamiltonian consisting of a charged two level fluctuator (see Table I for the microscopic parameters of the TLF) coupled to a CPB.

FIG. 4: Measured excess charge spectrum at relatively large microwave drive amplitudes near two of the more prominent avoided level crossings. (a) Measured spectrum between 33 and 34.6 GHz with $E_J/k_B= 0.95$ K (same avoided level crossing as in Fig. 3). (b) Same as (a) with the predicted spectrum from our system Hamiltonian (red dashed curve) using the parameters in Fig. 3 and Table I and observed local peaks in the spectrum due to the TLF as the blue points. (c) Measured spectrum between 43 and 44.5 GHz at $E_J/k_B= 0.1$ K. (d) Same as (c) with predicted spectrum (red dashed curve) using the parameters in Table I and observed local peaks in the spectrum due to the TLF as the blue points.

FIG. 5: (Color online) Measured decay rate (Γ_1) at $E_J/k_B = 0.1$ K as a function of energy level separation after first cooldown (blue triangles) and after the device was warmed up to room temperature and cooled back down to $T = 40$ mK (red circles). The observed peaks in Γ_1 before annealing (20, 34, 39, and 43 GHz) and after annealing (23 GHz) correlate with the location of observed avoided level crossings (see Table I).

TABLE I: Parameters of observed TLFs. N is the TLF number, f is the frequency near where the avoided level crossing occurs, $n_g^{-/+}$ is the negative and positive reduced gate voltage location of each TLF and $\Delta^{-/+}$ represents the splitting size of the crossing at $n_g^{-/+}$ for the specified value E_J . $(\varepsilon_b - \varepsilon_a)$ is the asymmetry in the potential energy of the TLF in the two wells, $Q\delta x \cos(\eta)/ed$ is the coupling between the TLF and the CPB and T_{ab} is the tunneling term between the two potential wells.

N	f (GHz)	n_g^-	Δ^- (MHz)	n_g^+	Δ^+ (MHz)	E_J/k_B (K)	$(\varepsilon_b - \varepsilon_a)/k_B$ (K)	$Q_{TLF}\delta x \cos(\eta)/ed$	T_{ab}/k_B (K)
1	20	-0.60	30	0.63	10	0.3	0.75	-0.032	0.3
2	34	-0.43	140	0.48	80	1.0	1.43	-0.074	0.39
3 ^a	39	-0.34	-	0.36	-	1.1	1.86 - 1.89	-0.083	< 0.17
4	43	-0.26	120	0.25	220	1.1	1.61	0.083	0.65
5 ^b	23	-0.57	90	0.58	140	0.55	0.34	0.078	0.52

^aThe splitting size was too small to resolve.

^bAfter annealing device at $T = 300$ K for 14 days.

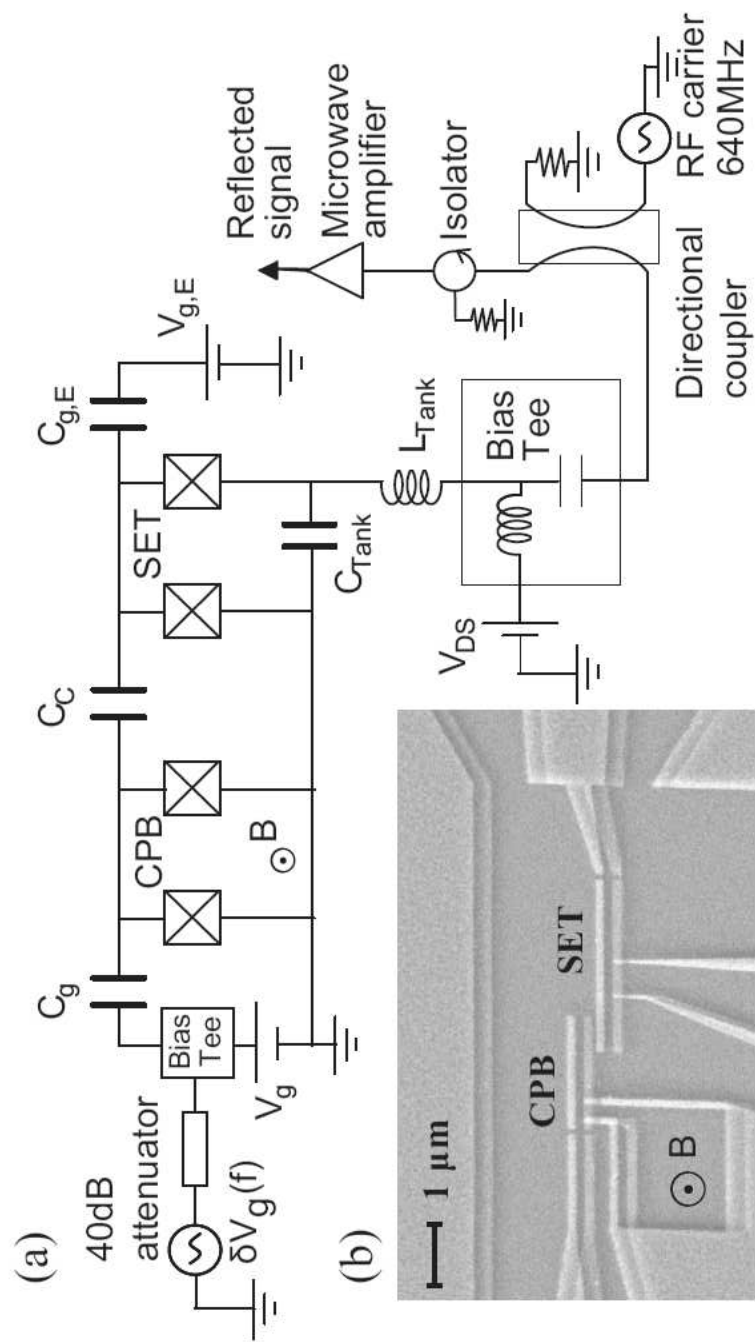


Fig. 1. Z. Kim *et al.*

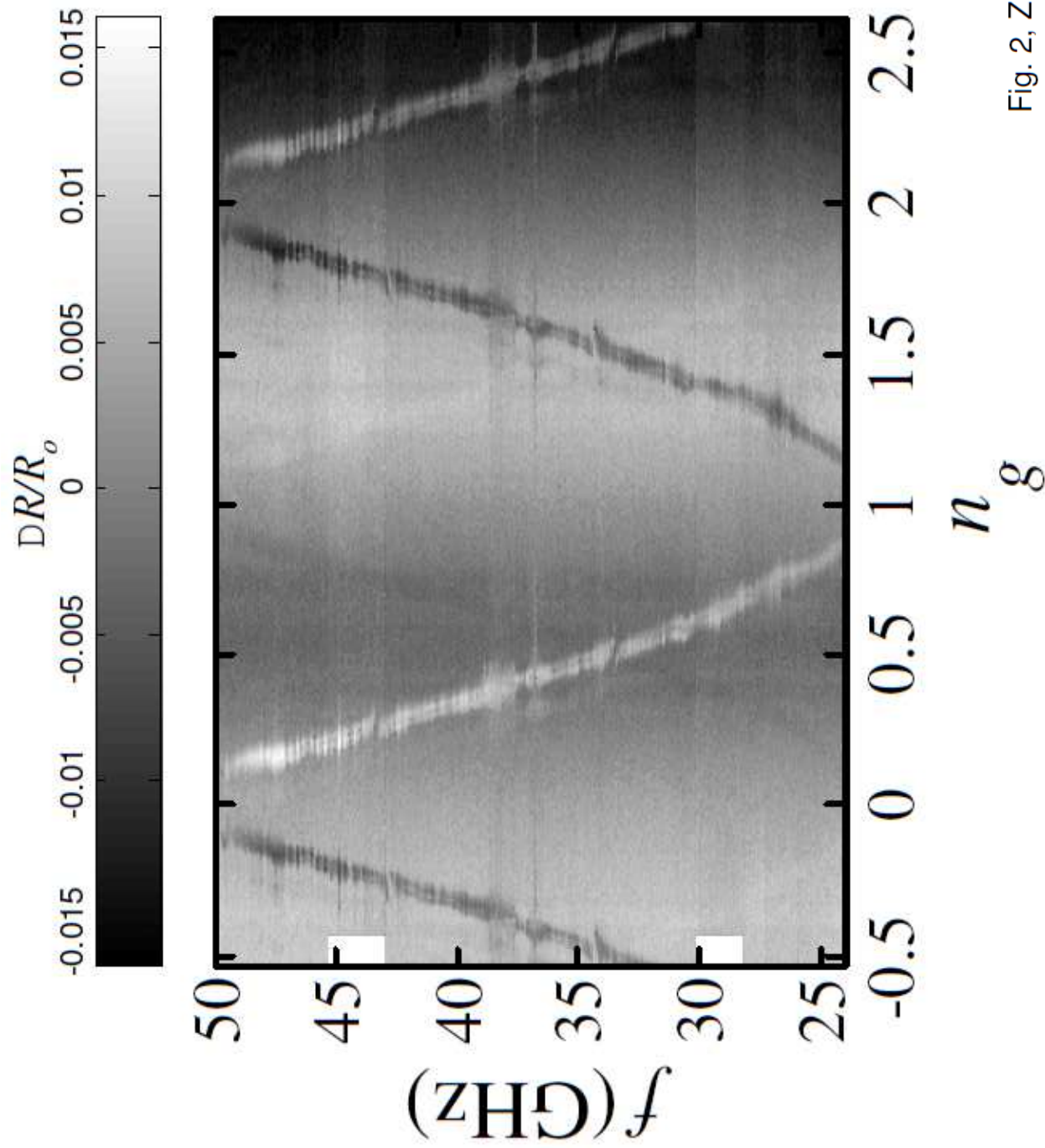


Fig. 2, Z. Kim e

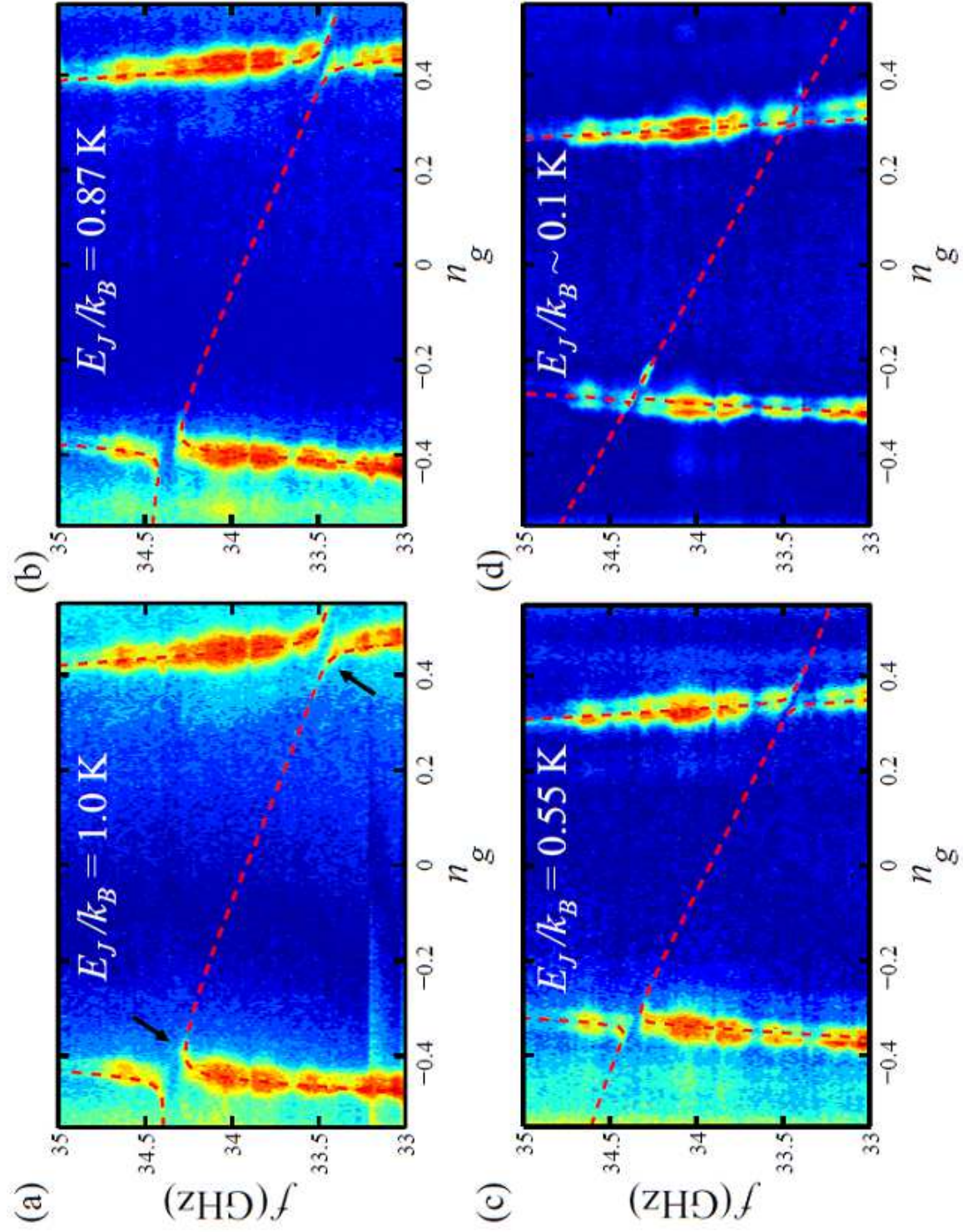


Fig. 3, Z. Kim *et al.*

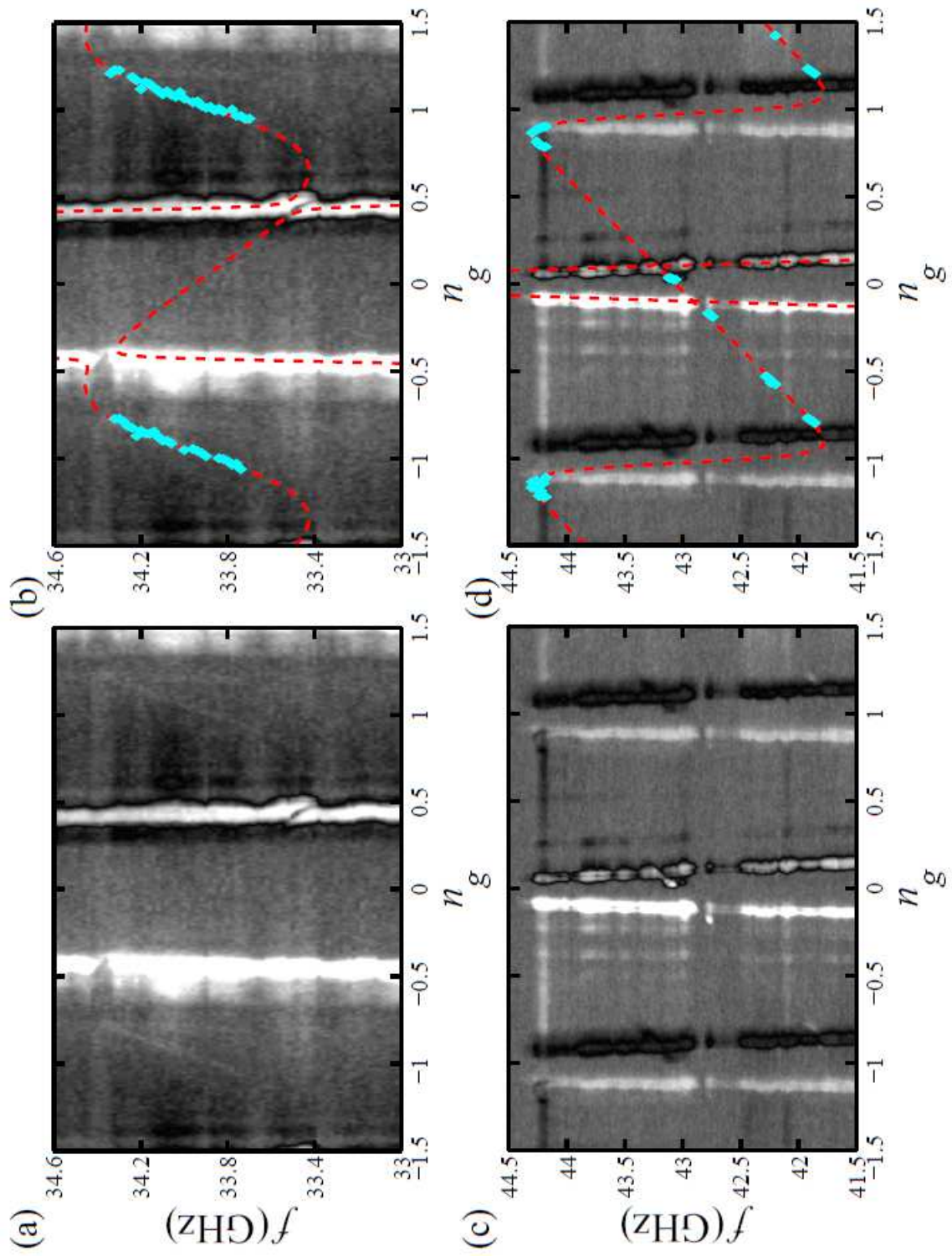


Fig. 4, Z. Kim et al.

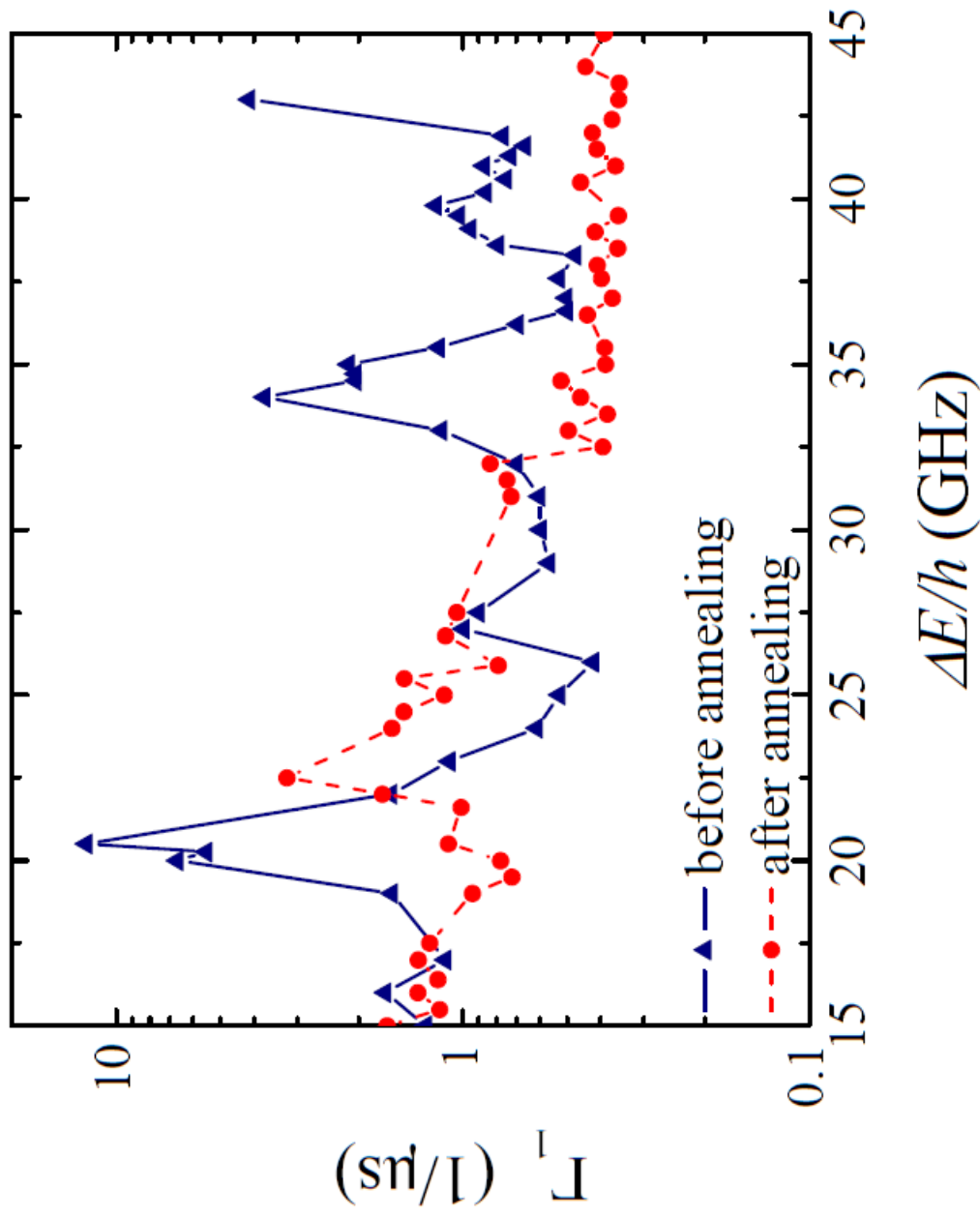


Figure 5, Z. Kim et al.